Published as: *Stem Cells*. 2013 August ; 31(8): 1563–1573.

Fetal deficiency of Lin28 programs life-long aberrations in growth and glucose metabolism

Gen Shinoda[1,2], **Ng Shyh-Chang**[1,2,3,5,6], **T. Yvanka de Soysa**[1,2], **Hao Zhu**[1,2,†], **Marc T. Seligson**[1,2], **Samar P. Shah**[1,2], **Nora Abo-Sido**[1,2], **Akiko Yabuuchi**[1,2], **John P. Hagan**[1,2,3,4], **Richard I. Gregory**[1,2,3], **John M. Asara**[5,6], **Lewis C. Cantley**[5,6], **Eric G. Moss**[7], and **George Q. Daley**[1,2,3,8,9,10,*]

[1]Stem Cell Transplantation Program, Stem Cell Program, Division of Pediatric Hematology/Oncology, Boston Children's Hospital, Boston, MA, USA

[2]Harvard Stem Cell Institute, Boston, MA, USA

[3]Department of Biological Chemistry and Molecular Pharmacology, Harvard Medical School, Boston, MA, USA

[4]Department of Molecular Virology, Immunology and Medical Genetics, The Ohio State University Medical Center, Columbus, OH, USA

[5]Division of Signal Transduction, Beth Israel Deaconess Medical Center, Boston, MA, USA

[6]Department of Medicine, Harvard Medical School, Boston, MA, USA

[7]Department of Molecular Biology, The University of Medicine and Dentistry of New Jersey, Newark, NJ, USA

[8]Division of Hematology, Brigham and Women's Hospital, Boston, MA, USA

[9]Howard Hughes Medical Institute, Boston, MA, USA

[10]Manton Center for Orphan Disease Research, Boston, MA, USA

Abstract

LIN28A/B are RNA binding proteins implicated by genetic association studies in human growth and glucose metabolism. Mice with ectopic over-expression of *Lin28a* have shown related phenotypes. Here we describe the first comprehensive analysis of the physiologic consequences of *Lin28a* and *Lin28b* deficiency in knockout (KO) mice. *Lin28a/b*-deficiency led to dwarfism starting at different ages, and compound gene deletions showed a cumulative dosage effect on organismal growth. Conditional gene deletion at specific developmental stages revealed that fetal

[*]To Whom Correspondence should be addressed: George Q. Daley, Children's Hospital Boston, One blackfan circle, Karp Building, 7th Floor, Boston, MA 02115, USA, Phone (617) 919-2013, Fax (617) 730-0222, george.daley@childrens.harvard.edu.
[†]Current address: Children's Research Institute, Departments of Pediatrics and Internal Medicine, University of Texas Southwestern Medical Center, Dallas, TX, USA.

AUTHOR CONTRIBUTIONS
G.S. conception and design, collection and/or assembly of data, data analysis and interpretation, manuscript writing and final approval of manuscript. N.S.C. collection and/or assembly of data, and data analysis and interpretation. T.Y.S., H.Z., M.T.S., S.P.S., and N.A.S. collection and/or assembly of data. A.Y., J.P.H., R.I.G., and E.G.M. provision of study materials. J.M.A. collection and/or assembly of data, data analysis and interpretation. L.C.C. data analysis and interpretation. G.Q.D. conception and design, data analysis and interpretation, manuscript writing and final approval of manuscript.

DISCLOSURE OF POTENTIAL CONFLICTS OF INTEREST
The authors declare no competing financial interests.

SUPPLEMENTAL INFORMATION
Supplemental Information includes nine figures and one table can be found with this article online.

but neither neonatal nor adult deficiency resulted in growth defects and aberrations in glucose metabolism. Tissue-specific KO mice implicated skeletal muscle-deficiency in the abnormal programming of adult growth and metabolism. The effects of *Lin28b* KO can be rescued by *Tsc1* haplo-insufficiency in skeletal muscles. Our data implicate fetal expression of *Lin28a/b* in the regulation of life-long effects on metabolism and growth, and demonstrate that fetal *Lin28b* acts at least in part via mTORC1 signaling.

Keywords

Lin28a; Lin28b; dwarfism; growth; glucose metabolism; diabetes; let-7; mTOR

INTRODUCTION

Organismal growth is a highly complex process tied to multiple genetic, nutritional, hormonal, and environmental factors. Recent human genome-wide association studies (GWAS) have reported over a hundred loci relevant to height [1–3]. Among these loci are genes encoding the RNA-binding protein *LIN28B*, which together with its paralog *Lin28A* regulate biogenesis of the *let-7* family of tumor-suppressor microRNAs, as well as mRNA stability and translation via direct binding of various gene transcripts such as the stem cell factor *Oct4*, the growth factor *Igf2,* cell cycle regulators and ribosomal subunits [4–11]. In addition to *Lin28B*, genetic variation around loci for at least three validated *let-7* targets (Dot1L, HMGA2, and CDK6) has also been associated with human height in Genome Wide Association Studies [1], and GWAS has also implicated *Lin28B* in the timing of onset of human puberty [12–15]. Interestingly, *lin-28* and *let-7* were originally identified as heterochronic regulators of developmental timing in *C. elegans* [16–18]. Whereas *lin-28* controls *let-7* biogenesis, *let-7* also regulates *lin-28* expression by binding its complementary sequences in the 3' untranslated region. Thus, *lin-28* and *let-7* regulate each other and comprise a double negative feedback loop. Their expression is tightly regulated during development, and evolutionarily conserved among worms, flies, frogs and mammals [19–21].

We have recently shown that transgenic mice which constitutively overexpress *Lin28a* manifest increased body size and delayed onset of puberty [22], and that overexpression of both murine *Lin28a* and human *LIN28B* promote an insulin-sensitized state that resists diabetes in mice, in direct contrast to overexpression of *let-7,* which results in insulin resistance and impaired glucose tolerance [23]. Given that *Lin28a/b* are expressed in distinct spatio-temporal patterns, their precise physiological roles in mammalian development and metabolism remain unclear. Here, we describe *Lin28a* and *Lin28b* knockout (KO) mice and characterize the distinct spatio-temporal functions of the *Lin28* paralogs.

MATERIALS AND METHODS

Mice

All animal procedures were approved by the Institutional Animal Care and Use Committee. Design of conditional *Lin28a* knockout mice was reported previously [23]. Design of conditional *Lin28b* knockout mice is shown in Supplemental Fig. 10. For *Lin28a* and *lin28b* conditional KO mice, PCR fragments of both gene loci were cloned into a plasmid having 2 loxP cassetes and a PGK-Neo cassete flanked with frt sequences, and targeting was performed into V6.5 embryonic stem (ES) cells. Homologous recombination was confirmed by Southern blotting. Chimeric mice were generated by injection of ES cells into Balb/c blastocysts, and then bred to Balb/c females to generate germline-transmitted pups. To delete the floxed allele in the germ line, we used a *Ddx4-Cre* strain (The Jackson

Laboratory). *LSL-iLet-7* mice were generated by crossing *iLet-7* mice [23] and *ROSA26-rtTA-IRES-EGFP* mice [24]. *Ddx4-Cre, Myf5-Cre, Alb-Cre, Ins2-Cre, ubiquitin-Cre/ERT2* and *ROSA26-rtTA-IRES-EGFP* mice were purchased from The Jackson Labolatory. *Tsc1*$^{fl/fl}$ mice are kindly provided from Dr. David Kwiatkowski laboratory. For all experiments, littermate controls were used.

Histology

Tissue samples were fixed in 10% buffered formalin or Bouin's solution and embedded in paraffin.

Glucose and Insulin Tolerance Tests

Overnight-fasted mice were given i.p. glucose (2 mg/g body weight). For insulin tolerance test, 5 hr fasted mice were given 0.75 U insulin/kg body weight by i.p. injection (Humulin). Blood glucose was determined with a Lifescan One Touch glucometer.

Drug treatment

Tamoxifen (Sigma) was dissolved in corn oil at 20 mg/mL. To delete floxed alleles in E15.5 embryos, a dose of 0.1mg/g mouse weight was injected intraperitoneally once to the mothers. For 7 to 9 days old pups, a dose of 0.5 mg/g mouse weight was injected intraperitoneally once. For adult mice, a dose of 0.2 mg/g mouse weight was injected 5 times in consecutive days.

Quantitative RT-PCR

Total RNA was collected by TRIzol and reverse-transcribed. mRNA and microRNA expression were measured by quantitative PCR using the ΔΔCT method as described previously [23].

Targeted liquid-chromatography mass spectrometry (LC/MS/MS)

LC/MS/MS-based metabolomics analysis was performed as described previously [25] Whole embryos were harvested in 80% (v/v) methanol at − 78°C. Insoluble material in lysates was centrifuged at 2,000g for 15 min, and the resulting supernatant was evaporated using a refrigerated speed vac. Samples were resuspended using 20 μL LC/MS grade water. 7 μL was injected and analyzed using a 5500 QTRAP triple quadrupole mass spectrometer (AB/SCIEX) coupled to a Prominence HPLC system (Shimadzu) using selected reaction monitoring (SRM) of a total of 252 endogenous water soluble metabolites for analyses of samples. Some metabolites were targeted in both the positive and negative ion mode for a total of 292 SRM transitions. ESI voltage was +4,900 V in the positive ion mode and −4,500 V in the negative ion mode using positive/negative switching. The dwell time was 4 ms per SRM transition, and the total cycle time was 1.82 sec producing 9–12 data points per metabolite peak. Samples were delivered to the MS using hydrophilic interaction chromatography (HILIC) using a 4.6 mm internal diameter × 10 cm Amide XBridge column (Waters) at 300 μL/min. Mobile phase gradients were run starting from 85% buffer B (LC/MS grade acetonitrile) to 35% buffer B from 0–3 min; 35% buffer B to 0% buffer B from 3–12 min; 0% buffer B held from 12–17 min; 0% buffer B to 85% buffer B from 17–18 min; and 85% B held for 7 min to re-equilibrate the column. Buffer A was comprised of 20 mM ammonium hydroxide and 20 mM ammonium acetate in 95:5 water:acetonitrile (pH=9.0). Peak areas from the total ion current for each metabolite SRM transition were integrated using MultiQuant v2.0 software (AB/SCIEX).

Statistical analysis

Data is presented as mean ± SEM. Student's t test (two-tailed distribution, two-sample unequal variance), Fisher's exact probability test, or Chi-square test was used to calculate p values, with Mendelian ratios as the expected distribution where appropriate. Statistical significance is displayed as * $p < 0.05$ or ** $p < 0.01$.

RESULTS

Lin28a knockout mice manifest dwarfism beginning in embryogenesis

We first generated and analyzed *Lin28a* KO mice (See Materials and Methods). *Lin28a* KO mice showed dwarfism as early as E13.5, and by E18.5 showed 20% reduction in weight, relative to heterozygote controls (Fig. 1A and 1B). Although born in the expected Mendelian ratio, over 93% of *Lin28a* KO mice died within 1 day after birth (Fig. 1C and 1D). By histopathologic analysis, 2 out of 5 KO mice which died perinatally harbored a cardiac ventricular septal defect (Supplementary Fig. 1A), but virtually all other tissues were histologically normal (Supplementary Fig. 1B). The high perinatal lethality remains unexplained.

Because a minority of KO mice survive to adulthood (Fig. 1D), we were able to analyze the postnatal growth of the survivors (Supplementary Fig. 2A). Both male and female KO mice were 30–50% smaller in weight and 20–30% shorter in length, and remained smaller than heterozygote controls throughout the observation period (Fig. 1E and 1F). Organ weights were proportionally lower relative to total body weight, except for fat mass, which was severely decreased in the adult KO mice (Fig. 1G). Dual-energy X-ray absorptiometry imaging confirmed the decreased fat mass and also revealed decreased bone mineral density in the KO animals (Fig. 1H and 1I, Supplementary Fig. 2B), suggesting that *Lin28a* KO mice suffer from metabolic dysregulation.

Lin28b regulates adult growth in males, but not in females

We next generated and analyzed *Lin28b* KO mice, using a similar gene deletion strategy as for *Lin28a* KO mice, in which exon 2 encoding the functional cold shock domain was engineered to be flanked by LoxP sites and subsequently deleted by Cre recombinase (See Materials and Methods). Although *LIN28B* is highly expressed in the placenta [26], we did not observe any difference in weights of *Lin28b* KO embryos or placentae at E18.5 relative to heterozygote controls, indicating that unlike *Lin28a, Lin28b* is dispensable for embryonic growth (Supplementary Fig. 3A and 3B). However, *Lin28b* KO males did show postnatal dwarfism, (Fig. 2A and 2B), with organ weights reduced in relative proportion to total body weight (Supplementary Fig. 3C). In contrast, *Lin28b* KO females showed no postnatal growth defects, suggesting *Lin28b* regulates growth in mice in a gender-specific manner.

Combined dosage of *Lin28a/b* is critical for postnatal growth

Lin28a and *Lin28b* are functionally redundant in that they both block biogenesis of *let-7* miRNAs and serve as oncogenes [4, 8, 27–29], although the precise mechanism of let-7 repression has been reported to be distinct for Lin28 paralogs [30]. To discern the importance of gene dosage of *Lin28a/b* on growth phenotypes, we bred $Lin28a^{+/-}b^{-/-}$ mice and examined their progenies. Weights of embryos and placentae at E13.5 were not significantly different between $Lin28a^{+/-}b^{-/-}$ and $Lin28a^{+/+}b^{-/-}$ (i.e. *Lin28b* KO) mice (Supplementary Fig. 3D). However, in both males and females, $Lin28a^{+/-}b^{-/-}$ mice showed postnatal dwarfism compared to *Lin28b* KO littermates (Fig. 2C and 2D). Haploinsufficiency of *Lin28a* affected postnatal growth only in a *Lin28b* null background, since $Lin28a^{+/-}$ mice grew comparably to $Lin28a^{+/+}$ (i.e. wild type) controls (Supplementary Fig. 3E), indicating that the combined dose of *Lin28a/b* alleles is critical to postnatal growth.

Lin28a/b double KO causes developmental delay and embryonic lethality

To discern the embryonic phenotypes of dual deficiency of *Lin28a/b,* we analyzed mid-gestation embryos at different ages and found that double KO (DKO) embryos were smaller in size at E9.5 and E10.5 compared to *Lin28a*$^{+/+}$ *b*$^{-/-}$ and *Lin28a*$^{+/-}$ *b*$^{-/-}$ embryos (Fig. 3A). Moreover, we observed significantly fewer somites by E10.5 in DKO embryos, suggesting a developmental delay (Fig. 3B). Open neural tubes were found in 2/7 E11.5 DKO embryos, which was also consistent with a developmental delay (Fig. 3C and 3D). Other abnormalities included collapsed ventricles and poor development of the forebrain in some cases. DKO embryos died between E10.5 and E12.5 (Fig. 3E and Supplementary Table).

Fetal expression of *Lin28a/b* is required for regulating postnatal growth

Lin28a and *Lin28b* are expressed in early embryos but in limited tissues in adults [31]. To test whether embryonic or adult expression regulates postnatal animal growth, we generated tamoxifen-inducible conditional KO mice by crossing a *ubiquitin-Cre/ERT2* expressing strain (*UBC-CreER*) lacking either *Lin28a* or *Lin28b* to a strain carrying floxed *Lin28a*$^{fl/fl}$ or *Lin28b*$^{fl/fl}$ alleles, to generate *Lin28a***$^{fl/-}$*; UBC-CreER (+)* or *Lin28b*$^{fl/-}$*; UBC-CreER (+)* mice (Fig. 4A and 4E). We injected tamoxifen (TAM) to delete the floxed alleles at different ages. PCR analysis confirmed high efficiency allele deletion in multiple tissues (Supplementary Fig. 4). For *Lin28a, Lin28a*$^{fl/-}$*; UBC-CreER (+)* males injected with TAM at E15.5 showed significant postnatal dwarfism, as measured by total body weight and body length (Fig. 4B and Supplementary Fig. 5A), although the degree of dwarfism at 3 wks old is more modest than in constitutive *Lin28a* KO mice. *Lin28a*$^{fl/-}$*; UBC-CreER (+)* females injected with TAM at E15.5 showed no dwarfism phenotype. In contrast, when TAM was injected at 7–9 days (neonate) or 6 weeks of age (adult), their subsequent adult growth was indistinguishable from controls (Fig. 4C–D and Supplementary Fig. 5B–C). For *Lin28b, Lin28b*$^{fl/-}$*; UBC-CreER (+)* males injected with TAM at E15.5 phenocopied the postnatal dwarfism of constitutive *Lin28b* KO mice (Fig. 4F and Supplementary Fig. 5D). In contrast, no growth phenotype was observed when TAM was injected at 7–9 days (neonate) or 6 weeks old (adult) into *Lin28b*$^{fl/-}$*; UBC-CreER (+)* males (Fig. 4G–H and Supplementary Fig. 5E–F). These results demonstrate that postnatal growth is dictated by fetal expression of both *Lin28a* and *Lin28b*, whereas adult expression is dispensable. Interestingly, deletion of *Lin28a* at E15.5 does not result in the high frequency of perinatal death observed in constitutive *Lin28a* KO, nor does it phenocopy the full degree of dwarfism due to constitutive loss of *Lin28a*, whereas deletion of fetal *Lin28b* at E15.5 fully phenocopies the dwarfism due to constitutive loss of *Lin28b.* Taken together, our data suggests that *Lin28a* acts earlier on organismal growth than *Lin28b,* such that effects of gene deletion are already apparent *in utero*.

Lin28a KO and *Lin28b* KO mice suffer from defects in glucose metabolism

We have previously shown that *Lin28a* and *LIN28B* transgenic mice are more resistant to diabetes whereas muscle-specific *Lin28a* KO mice show insulin resistance and impaired glucose uptake [23]. In the present study, we found that *Lin28a* KO mice show a dramatic loss of fat mass by adulthood (Fig. 1G–H), although we detect no Lin28a/b expression in fat tissues (Supplementary Fig. 6). Thus we further investigated whether *Lin28a/b* play systemic physiological roles in programming metabolism prior to changes in growth. Glucose tolerance tests (GTT) and insulin tolerance tests (ITT) demonstrated that muscle-specific loss of *Lin28b* as well as *Lin28a* [23] led to insulin resistance and impaired glucose uptake (Fig. 5A and 5B). Since *Lin28a* KO mice already show a significant growth delay as early as E13.5, we performed metabolomic profiling at E10.5 to determine if loss of *Lin28a* affects embryonic metabolism prior to detectable differences in embryonic growth. We observed a relative accumulation of glucose-6-phosphate and fructose-6-phosphate, and significant decreases in glycolytic intermediates after the phosphofructokinase step,

HHMI Author Manuscript

HHMI Author Manuscript

suggesting a lower flux in glycolysis (Fig. 5C). This is consistent with our observations of a lower NADH/NAD ratio, and a higher GSH/GSSG ratio, which are indicative of lower rates of glucose catabolism via glycolysis, Krebs cycle and oxidative phosphorylation, which generate NADH and reactive oxygen species (Fig. 5D). We also found an aberrant drop in dUTP and an accumulation of dTTP, dTDP, dTMP and thymine, suggesting that loss of *Lin28a* also leads to dysregulation of pyrimidine metabolism (Fig. 5E).

Fetal muscle-specific expression of *Lin28b* regulates adult growth

Mice engineered to over-express *let-7* miRNA are smaller than controls [23, 32]. To understand how *Lin28a* and *Lin28b* deficiency affect *let-7* levels, we compared *let-7* expression levels by quantitative PCR in E8.5 embryos and various tissues of neonatal and adult mice. *Lin28a* but not *Lin28b* KO mice expressed 7- to 18-fold higher levels of *let-7a, d, e, f, g, and i but for unclear reasons not b or c,* relative to wild-type controls in the E8.5 embryo (Fig. 6A), indicating that *Lin28a* is the primary regulator of *let-7* microRNAs in the early embryo. *Let-7* was also higher in the skeletal muscles of neonatal *Lin28a* KO mice, but no increases in *let-7* were observed in adult skeletal muscles nor any other tissue (Fig. 6B and Supplementary Fig. 7A). This result is consistent with the fact that Lin28a is primarily restricted in its expression to fetal tissues. For *Lin28b* KO mice, some *let-7* family members were expressed at modestly higher levels in adult skeletal muscles in *Lin28b* KO mice (1.3- to 2-fold; Fig. 6C and Supplementary Fig. 7B). These observations indicate that *Lin28a* potently suppresses *let-7* biogenesis during embryogenesis, but its effect decreases postnatally and eventually disappears by adulthood, whereas *Lin28b* has a smaller but still significant effect on *let-7* biogenesis in adulthood, indicating that *Lin28a* and *Lin28b* regulate *let-7* biogenesis and growth at different developmental stages.

Our previous paper reported that *iLet-7* mice, in which a *Lin28*-resistant form of *let-7g* is induced with doxycycline, manifest growth retardation if *let-7g* is induced globally from three weeks of age onward [23]. To determine if skeletal muscle-specific *let-7* regulates organismal growth, we generated *LSL-iLet-7* mice, in which Cre recombinase removes a Lox-Stop-Lox cassette, thereby enabling tissue-specific *let-7g* induction with doxycycline (See Materials and Methods). We crossed *LSL-iLet-7* mice with skeletal muscle specific *Myf5-Cre* mice, and documented 6 fold more expression of the transgenic *let-7g* in neonatal skeletal muscle relative to controls (data not shown). Upon induction with doxycycline from conception onward we observed postnatal dwarfism in both males and females, demonstrating that overexpression of *let-7* in skeletal muscle is sufficient to cause growth retardation (Fig. 6D and 6E and Supplementary Fig. 7C and 7D).

Furthermore, to determine if the differences in skeletal muscle *let-7* between *Lin28a* and *Lin28b* KO mice were important for animal growth, we bred skeletal muscle specific *Myf5-Cre* mice to *Lin28a*$^{fl/fl}$ or *Lin28b*$^{fl/fl}$ mice. Whereas muscle-specific *Lin28a* KO mice (*Lin28a*$^{fl/fl}$*; Myf5-Cre+)* were comparable in size to control *Lin28a*$^{fl/fl}$ mice (Supplementary Fig. 7E), muscle-specific *Lin28b* KO (*Lin28b*$^{fl/fl}$*; Myf5-Cre+)* males were smaller than control *Lin28b*$^{fl/fl}$ males, and phenocopied the dwarfism in constitutive *Lin28b* KO males (Fig. 6F and 6G, compared to Fig. 2A and 2B). Notably, both *Lin28a* KO and *Lin28b*$^{fl/fl}$*; Myf5-Cre+* muscles showed normal histology (Supplementary Fig. 1B and 7F), comparable abundance of fast twitch (type II myosin) muscle fibers, and comparable mitochondrial DNA content and mitochondrial gene expression to controls (Supplementary Fig. 8). In contrast, liver- or pancreatic β cell-specific *Lin28b* KO did not affect adult growth (Supplementary Fig. 9). Our results indicate that absence of *Lin28b* in the fetal skeletal muscle is sufficient to dysregulate adult growth, whereas *Lin28a* must be lacking in additional tissues to manifest a change in adult growth.

Lin28b acts through Tsc1-mTOR signaling in skeletal muscle

We have previously shown that *Lin28a* and *LIN28B* regulate glucose metabolism at least in part via *let-7* and the insulin-PI3K-mTOR pathway [23]. *Tsc1* is a suppressive regulator of the mTORC1 signaling [33]. Haploinsufficiency of *Tsc1* activates mTORC1 signaling. *Tsc1* KO mice die during embryonic development, whereas *Tsc1*$^{+/-}$ mice are viable with increased tumor-susceptibility in various organs [34]. We hypothesized that activation of mTORC1 signaling via *Tsc1* haploinsufficiency might rescue the dwarfism of *Lin28b* KO mice, and thus we crossed *Tsc1*$^{+/-}$ mice to *Lin28b*$^{+/-}$ or *Lin28b*$^{-/-}$ mice and tracked their growth. The growth of *Lin28b*$^{-/-}$*; Tsc1*$^{+/-}$ males was significantly improved compared to *Lin28b* KO mice, and comparable to that of *Lin28b*$^{+/-}$ mice (Fig. 7A and 7B). By contrast, *Lin28b*$^{+/-}$*; Tsc1*$^{+/-}$ mice showed no growth advantage relative to *Lin28b*$^{+/-}$ mice, indicating that the effects of *Lin28b* deficiency on postnatal growth could be reversed by enhancing mTORC1 signaling. Interestingly, we likewise generated *Lin28a*$^{-/-}$*; Tsc1*$^{+/-}$ mice but found that *Tsc1* haploinsufficiency failed to rescue the dwarfism and perinatal lethality phenotypes seen with constitutional *Lin28a* deficiency.

Next, we tested the hypothesis that *Lin28b/Tsc1* effects on growth are skeletal muscle specific. We generated *Lin28b fl/fl; Tsc1 fl/+; Myf5-Cre* mice, in which *Lin28b* KO and *Tsc1* haploinsufficiency are achieved only in skeletal muscles. *Tsc1* haploinsufficiency in skeletal muscles partially rescued the postnatal dwarfism phenotype seen in skeletal muscle specific *Lin28b* KO mice (Fig. 7C and 7D). Moreover, GTT demonstrated modest but significant improvement in *Lin28b fl/fl; Tsc1 fl/+; Myf5-Cre* mice compared to *Lin28b fl/fl; Myf5-Cre* mice (Fig. 7E). Taken together, our results suggest that *Lin28b* expression in fetal muscle programs adult metabolism and growth in part through the Tsc1-mTORC1 signaling pathway.

DISCUSSION

Heterochronic metabolism and the *Lin28a/b-mTOR* pathway

Both *lin-28* and *let-7* were originally identified in a *C. elegans* mutagenesis screen as heterochronic regulators of developmental timing. We and others have reported that overexpression of *Lin28a* and *let-7* affect organismal size [23, 32] and onset of puberty in mice and humans [12–15]. In searching for the mechanism of growth regulation, we found that mammalian *Lin28a/b* also regulate glucose metabolism, in part through the *let-7*-mediated repression of multiple components of the insulin-PI3K-mTOR pathway [23]. In this study, using genetic KO mouse models we have established that *Lin28a* and *Lin28b* are physiologically required for normal glucose homeostasis, albeit with distinct spatio-temporal patterns during mammalian development (Fig. 7F). Furthermore, we have found that fetal *Lin28a/b* exerts long-lasting effects on adult metabolism and growth, long after the normal expression patterns of these paralogs have extinguished in most tissues. Indeed, *Lin28a*$^{fl/-}$*; UBC-CreER (+)* or *Lin28b*$^{fl/-}$*; UBC-CreER (+)* mice revealed that when deleted in adulthood, *Lin28a* or *Lin28b* are entirely dispensable with regard to the persistent growth observed with organismal aging in mice. Long-standing adult growth and metabolic effects were observed without concomitant gross defects in mammalian development, nor a disproportionate decrease in tissue mass, save for fat, in which *Lin28a/b* are not expressed. We found that deficiency of *Lin28a/b* in fetal muscle dysregulates adult metabolism; although we observe no defects in muscle development. Our finding that haploinsufficiency of *Tsc1* can partially rescue the growth and glucose metabolism defects of *Lin28b* KO mice, further suggests that fetal *Lin28b*'s effects on adult metabolism are mediated, at least in part, by mTORC1 signaling. Loss of embryonic *Lin28a* led to a general dysregulation of glycolytic flux in early embryos before changes in growth were detected, consistent with previous findings that mTORC1 signaling directly regulates glucose metabolism [33].

Model of differential effects of *Lin28a* and *Lin28b* on postnatal growth

Although our results demonstrate that adult growth is altered by fetal but not adult deficiency of *Lin28a* or *Lin28b*, we observed important differences in the phenotypes mediated by temporal and tissue-specific deficiency of these closely related paralogs. Conditional deletion of *Lin28a* at E15.5 failed to phenocopy constitutive loss of *Lin28a*, which was associated with perinatal lethality and dwarfism, whereas *Lin28b* deletion at a similar stage fully phenocopied the dwarfism due to constitutive loss of *Lin28b.* Furthermore constitutive loss of *Lin28a* caused metabolic dysfunction and dwarfism in embryos, whereas constitutive loss of *Lin28b* did not influence metabolism until later in adults. These data suggest that *Lin28a* is relevant at an earlier embryonic stage of development than *Lin28b*, although both are relevant during mid-gestation as combined loss of both *Lin28a* and *Lin28b* led to synthetic lethality first noted around E10.5.

Fetal *Lin28a/b* and the Barker hypothesis

The “Barker hypothesis”, originally proposed two decades ago, holds that an epigenetic memory of poor fetal and infant nutrition causes permanent changes in metabolism and leads to increased risks in adult life for chronic metabolic diseases such as type 2 diabetes (T2D) [35, 36]. Epidemiological observations support the relationship between fetal metabolism and adult insulin resistance, and it is now generally accepted that environmental factors in early life play a major role in the pathogenesis of T2D [35, 36]. Our conditional KO mice and metabolomics studies here establish that deletion of *Lin28a/b* during fetal development dictates long-term effects on adult metabolism, resulting in increased insulin resistance and a diabetic phenotype, opposite to the enhanced glucose metabolism which we recently reported as a consequence of hyperfunction of *Lin28* in conditional transgenic murine models [23]. The *Lin28/let-7* axis thus represents a means by which fetal metabolic regulators can influence life-long growth and metabolism phenotypes. Although we have identified fetal muscle cells as key cellular targets of *Lin28* function, and the mTORC1 pathway in the molecular mechanism, how defects in fetal expression of the *Lin28/let-7* axis translates into the long-term epigenetic changes that influence adult metabolism remains a mystery. Our several strains of *Lin28a/b* knockout mice should provide powerful tools to study the fetal programming of adult metabolism, with relevance to the ongoing search for new medical interventions in chronic metabolic diseases.

Supplementary Material

Refer to Web version on PubMed Central for supplementary material.

Acknowledgments

We thank Mathew William Lensch for invaluable discussions and advice, David J. Kwiatkowski for *Tsc1* mice, and Roderick Bronson and the Harvard Medical School Rodent Histopathology Core for mouse tissue pathology. We also thank Min Yuan and Susanne Breitkopf for help with mass spectrometry experiments and grants NIH 5P01CA120964-04 and NIH DF/HCC Cancer Center Support Grant 5P30CA006516-46 (J.M.A.) The work was supported by grants from the Alex’s Lemonade Stand Foundation and the Ellison Medical Foundation to GQD. GQD is an affiliate member of the Broad Institute, and an investigator of the Howard Hughes Medical Institute and the Manton Center for Orphan Disease Research.

REFERENCES

1. Lettre G, Jackson AU, Gieger C, et al. Identification of ten loci associated with height highlights new biological pathways in human growth. Nat Genet. 2008; 40:584–591. [PubMed: 18391950]
2. Lango Allen H, Estrada K, Lettre G, et al. Hundreds of variants clustered in genomic loci and biological pathways affect human height. Nature. 2010; 467:832–838. [PubMed: 20881960]

3. Lanktree MB, Guo Y, Murtaza M, et al. Meta-analysis of Dense Genecentric Association Studies Reveals Common and Uncommon Variants Associated with Height. Am J Hum Genet. 2011; 88:6–18. [PubMed: 21194676]
4. Heo I, Joo C, Cho J, et al. Lin28 mediates the terminal uridylation of let-7 precursor MicroRNA. Mol Cell. 2008; 32:276–284. [PubMed: 18951094]
5. Newman MA, Thomson JM, Hammond SM. Lin-28 interaction with the Let-7 precursor loop mediates regulated microRNA processing. RNA. 2008; 14:1539–1549. [PubMed: 18566191]
6. Piskounova E, Viswanathan SR, Janas M, et al. Determinants of microRNA processing inhibition by the developmentally regulated RNA-binding protein Lin28. J Biol Chem. 2008; 283:21310–21314. [PubMed: 18550544]
7. Rybak A, Fuchs H, Smirnova L, et al. A feedback loop comprising lin-28 and let-7 controls pre-let-7 maturation during neural stem-cell commitment. Nat Cell Biol. 2008; 10:987–993. [PubMed: 18604195]
8. Viswanathan SR, Daley GQ, Gregory RI. Selective blockade of microRNA processing by Lin28. Science. 2008; 320:97–100. [PubMed: 18292307]
9. Polesskaya A, Harel-Bellan A. A novel role for an embryonic regulatory protein Lin-28 in adult skeletal muscle differentiation. Med Sci (Paris). 2007; 23:796–797. [PubMed: 17937883]
10. Qiu C, Ma Y, Wang J, et al. Lin28-mediated post-transcriptional regulation of Oct4 expression in human embryonic stem cells. Nucleic Acids Res. 2010; 38:1240–1248. [PubMed: 19966271]
11. Xu B, Zhang K, Huang Y. Lin28 modulates cell growth and associates with a subset of cell cycle regulator mRNAs in mouse embryonic stem cells. RNA. 2009; 15:357–361. [PubMed: 19147696]
12. Ong KK, Elks CE, Li S, et al. Genetic variation in LIN28B is associated with the timing of puberty. Nat Genet. 2009
13. Sulem P, Gudbjartsson DF, Rafnar T, et al. Genome-wide association study identifies sequence variants on 6q21 associated with age at menarche. Nat Genet. 2009
14. He C, Kraft P, Chen C, et al. Genome-wide association studies identify loci associated with age at menarche and age at natural menopause. Nat Genet. 2009; 41:724–728. [PubMed: 19448621]
15. Perry JR, Stolk L, Franceschini N, et al. Meta-analysis of genome-wide association data identifies two loci influencing age at menarche. Nat Genet. 2009; 41:648–650. [PubMed: 19448620]
16. Ambros V, Horvitz HR. Heterochronic mutants of the nematode Caenorhabditis elegans. Science. 1984; 226:409–416. [PubMed: 6494891]
17. Moss EG, Lee RC, Ambros V. The cold shock domain protein LIN-28 controls developmental timing in C. elegans and is regulated by the lin-4 RNA. Cell. 1997; 88:637–646. [PubMed: 9054503]
18. Reinhart BJ, Slack FJ, Basson M, et al. The 21-nucleotide let-7 RNA regulates developmental timing in Caenorhabditis elegans. Nature. 2000; 403:901–906. [PubMed: 10706289]
19. Nimmo RA, Slack FJ. An elegant miRror: microRNAs in stem cells, developmental timing and cancer. Chromosoma. 2009; 118:405–418. [PubMed: 19340450]
20. Moss EG, Tang L. Conservation of the heterochronic regulator Lin-28, its developmental expression and microRNA complementary sites. Dev Biol. 2003; 258:432–442. [PubMed: 12798299]
21. Schulman BR, Esquela-Kerscher A, Slack FJ. Reciprocal expression of lin-41 and the microRNAs let-7 and mir-125 during mouse embryogenesis. Dev Dyn. 2005; 234:1046–1054. [PubMed: 16247770]
22. Zhu H, Shah S, Shyh-Chang N, et al. Lin28a transgenic mice manifest size and puberty phenotypes identified in human genetic association studies. Nat Genet. 2010; 42:626–630. [PubMed: 20512147]
23. Zhu H, Shyh-Chang N, Segre AV, et al. The Lin28/let-7 axis regulates glucose metabolism. Cell. 2011; 147:81–94. [PubMed: 21962509]
24. Belteki G, Haigh J, Kabacs N, et al. Conditional and inducible transgene expression in mice through the combinatorial use of Cre-mediated recombination and tetracycline induction. Nucleic Acids Res. 2005; 33:e51. [PubMed: 15784609]

25. Yuan M, Breitkopf SB, Yang X, et al. A positive/negative ion-switching, targeted mass spectrometry-based metabolomics platform for bodily fluids, cells, and fresh and fixed tissue. Nat Protoc. 2012; 7:872–881. [PubMed: 22498707]

26. Guo Y, Chen Y, Ito H, et al. Identification and characterization of lin-28 homolog B (LIN28B) in human hepatocellular carcinoma. Gene. 2006; 384:51–61. [PubMed: 16971064]

27. Iliopoulos D, Hirsch HA, Struhl K. An epigenetic switch involving NF-kappaB, Lin28, Let-7 MicroRNA, and IL6 links inflammation to cell transformation. Cell. 2009; 139:693–706. [PubMed: 19878981]

28. Viswanathan SR, Powers JT, Einhorn W, et al. Lin28 promotes transformation and is associated with advanced human malignancies. Nat Genet. 2009; 41:843–848. [PubMed: 19483683]

29. West JA, Viswanathan SR, Yabuuchi A, et al. A role for Lin28 in primordial germ-cell development and germ-cell malignancy. Nature. 2009; 460:909–913. [PubMed: 19578360]

30. Piskounova E, Polytarchou C, Thornton JE, et al. Lin28A and Lin28B inhibit let-7 microRNA biogenesis by distinct mechanisms. Cell. 2011; 147:1066–1079. [PubMed: 22118463]

31. Yang DH, Moss EG. Temporally regulated expression of Lin-28 in diverse tissues of the developing mouse. Gene Expr Patterns. 2003; 3:719–726. [PubMed: 14643679]

32. Frost RJ, Olson EN. Control of glucose homeostasis and insulin sensitivity by the Let-7 family of microRNAs. Proc Natl Acad Sci U S A. 2011; 108:21075–21080. [PubMed: 22160727]

33. Laplante M, Sabatini DM. mTOR Signaling in Growth Control and Disease. Cell. 2012; 149:274–293. [PubMed: 22500797]

34. Kwiatkowski DJ, Zhang H, Bandura JL, et al. A mouse model of TSC1 reveals sex-dependent lethality from liver hemangiomas, and up-regulation of p70S6 kinase activity in Tsc1 null cells. Hum Mol Genet. 2002; 11:525–534. [PubMed: 11875047]

35. Hales CN, Barker DJ. Type 2 (non-insulin-dependent) diabetes mellitus: the thrifty phenotype hypothesis. Diabetologia. 1992; 35:595–601. [PubMed: 1644236]

36. Hales CN, Barker DJ. The thrifty phenotype hypothesis. Br Med Bull. 2001; 60:5–20. [PubMed: 11809615]

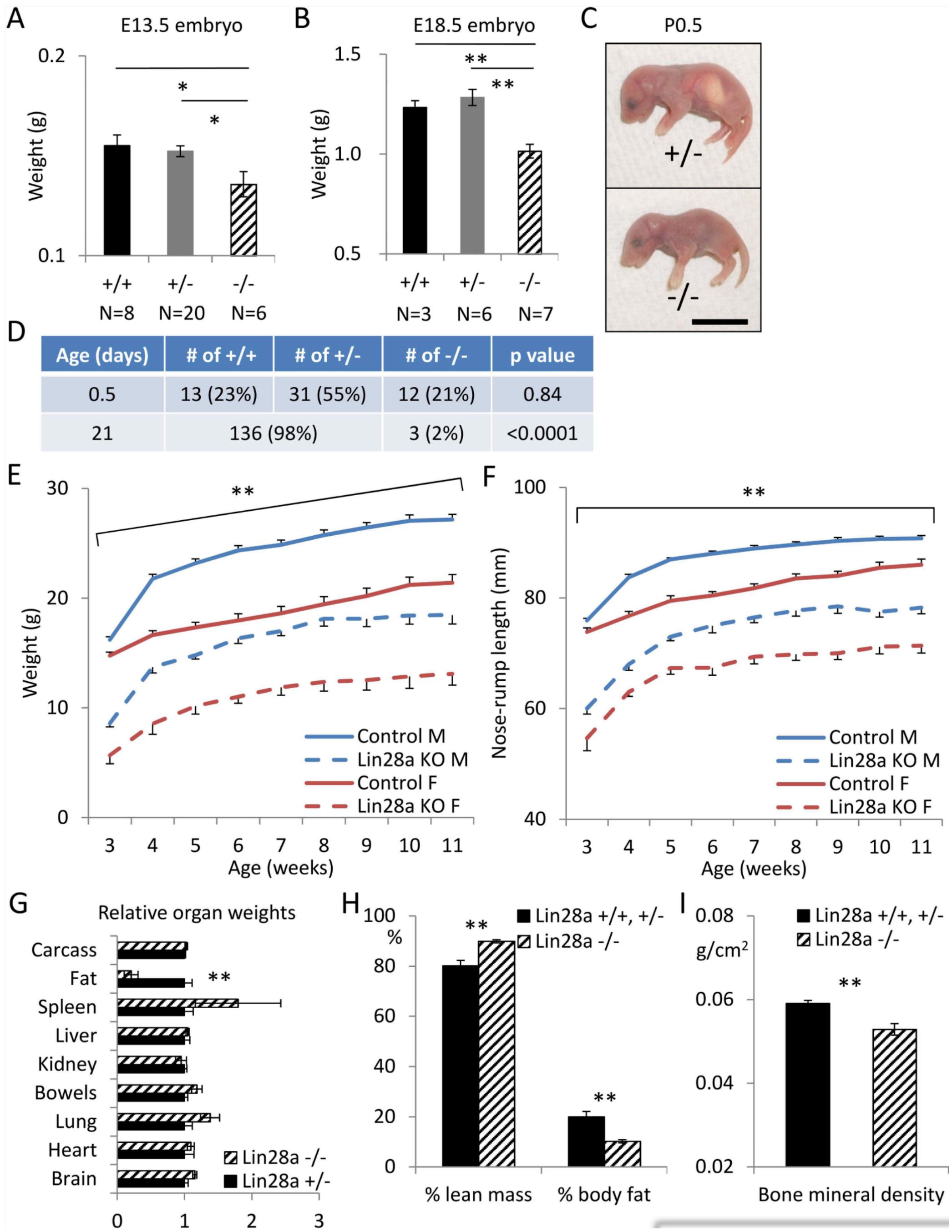

Figure 1. Constitutive deletion of *Lin28a* leads to persistent growth retardation from embryogenesis through adulthood

(A) Body weights of E13.5 *Lin28a +/+, +/−* and −/− embryos. (B) Body weights of E18.5 *Lin28a +/+, +/−* and −/− embryos. (C) Representative images of a heterozygous mouse and its *Lin28a* KO littermate. Bar 1cm. (D) Viability of P0.5 newborns and 21-day-old pups born from an inbreeding cross of *Lin28a* heterozygotes. P values were calculated by Chi-square test. (E–F) Growth curves for *Lin28a* heterozygous (solid) vs KO (dashed) mice, both male (blue) and female (red). N=4–15. (E) Body weight. (F) Body length. (G) Organ weights normalized to total body weight from 4 to 5-month-old males. Epididymal fat pads were used to measure the fat weight. N=3. (H) DEXA measurements of % lean and % fat weights, relative to total body weight. N=5–8. (I) DEXA measurement of bone mineral density. N=5–8. * $p<0.05$, ** $p<0.01$. Error bars represent SEM.

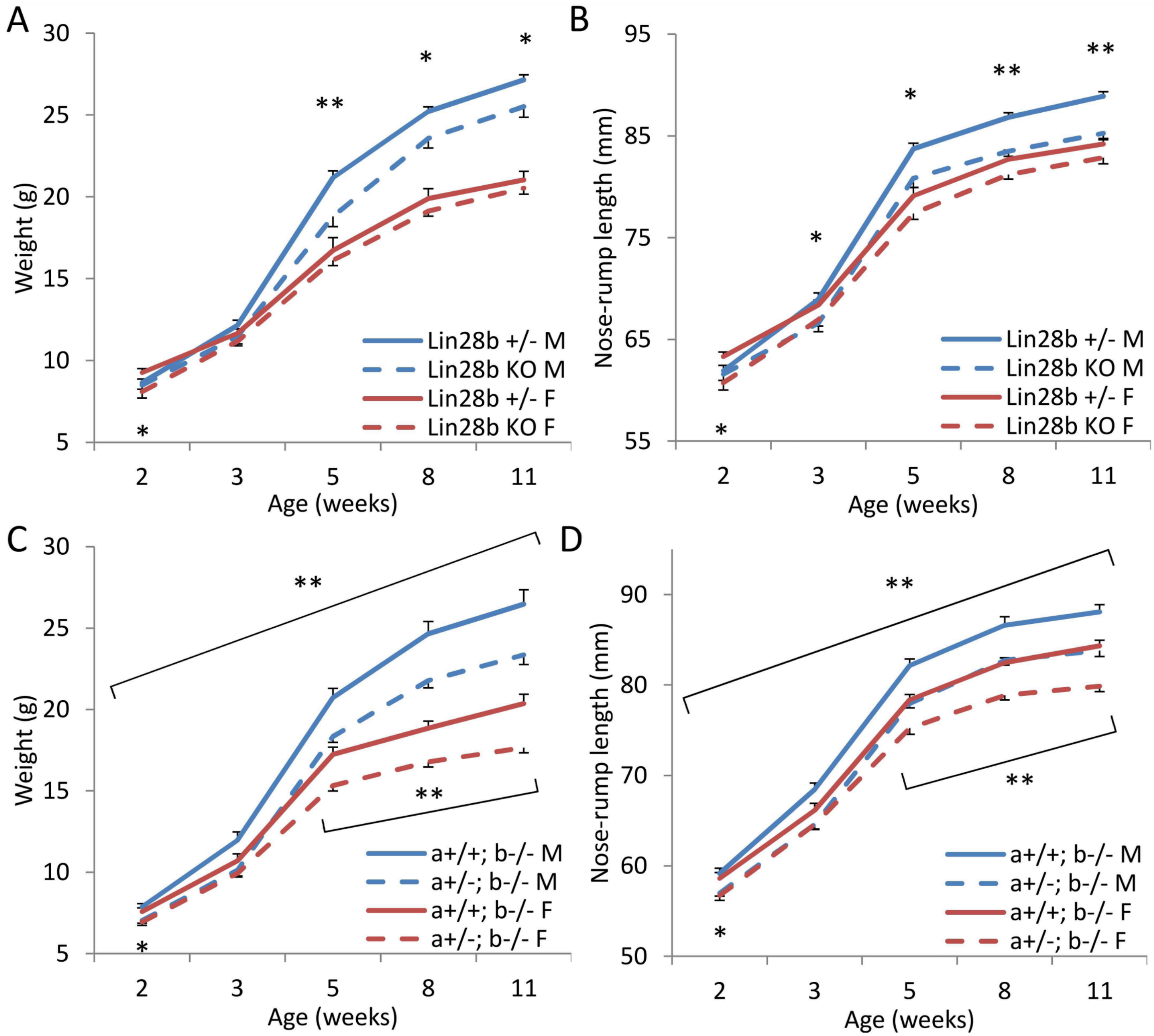

Figure 2. *Lin28a* and *Lin28b* dosage regulates postnatal growth

(A–B) Postnatal growth curves of *Lin28b* heterozygous vs. KO mice. N=8–21. (A) Body weight. (B) Body length. (C–D) Postnatal growth curves of *Lin28a* +/+ vs. +/− mice on a *Lin28b* KO background. N=11–22. (C) Body weight. (D) Body length. * p<0.05, ** p<0.01. Error bars represent SEM.

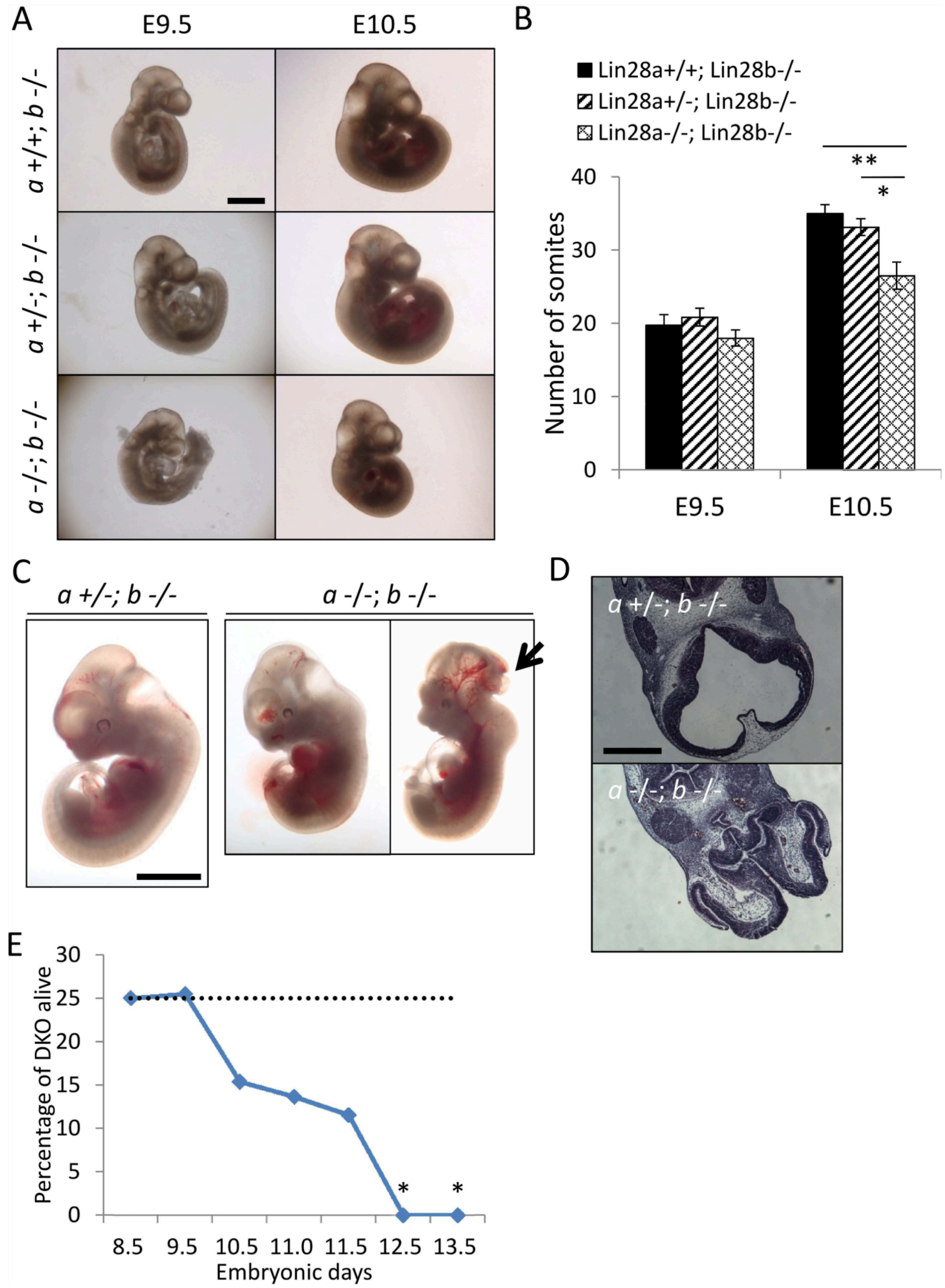

Figure 3. Double knockout of *Lin28a/b* leads to synthetic lethality in E10.5–E12.5 embryos

(A) Representative images, and (B) Number of somites, in *Lin28a +/+* vs. *Lin28a +/−* vs. *Lin28a −/−* embryos on a *Lin28b* KO background at E9.5–10.5. N=4–15. (C) Representative images of *Lin28a +/−* vs. *Lin28a −/−* embryos on a *Lin28b* KO background at E11.5. Arrow indicates an open neural tube. (D) Hematoxylin-eosin (H&E) staining of *Lin28a +/−* vs. *Lin28a −/−* embryos on a *Lin28b* KO background at E11.5. (E) Frequency of viable *Lin28a −/−; Lin28b −/−* embryos at different ages. See the Supplementary Table. Scale bars 1 mm (A and C), 500 μm (D). * p<0.05, ** p<0.01. Error bars represent SEM.

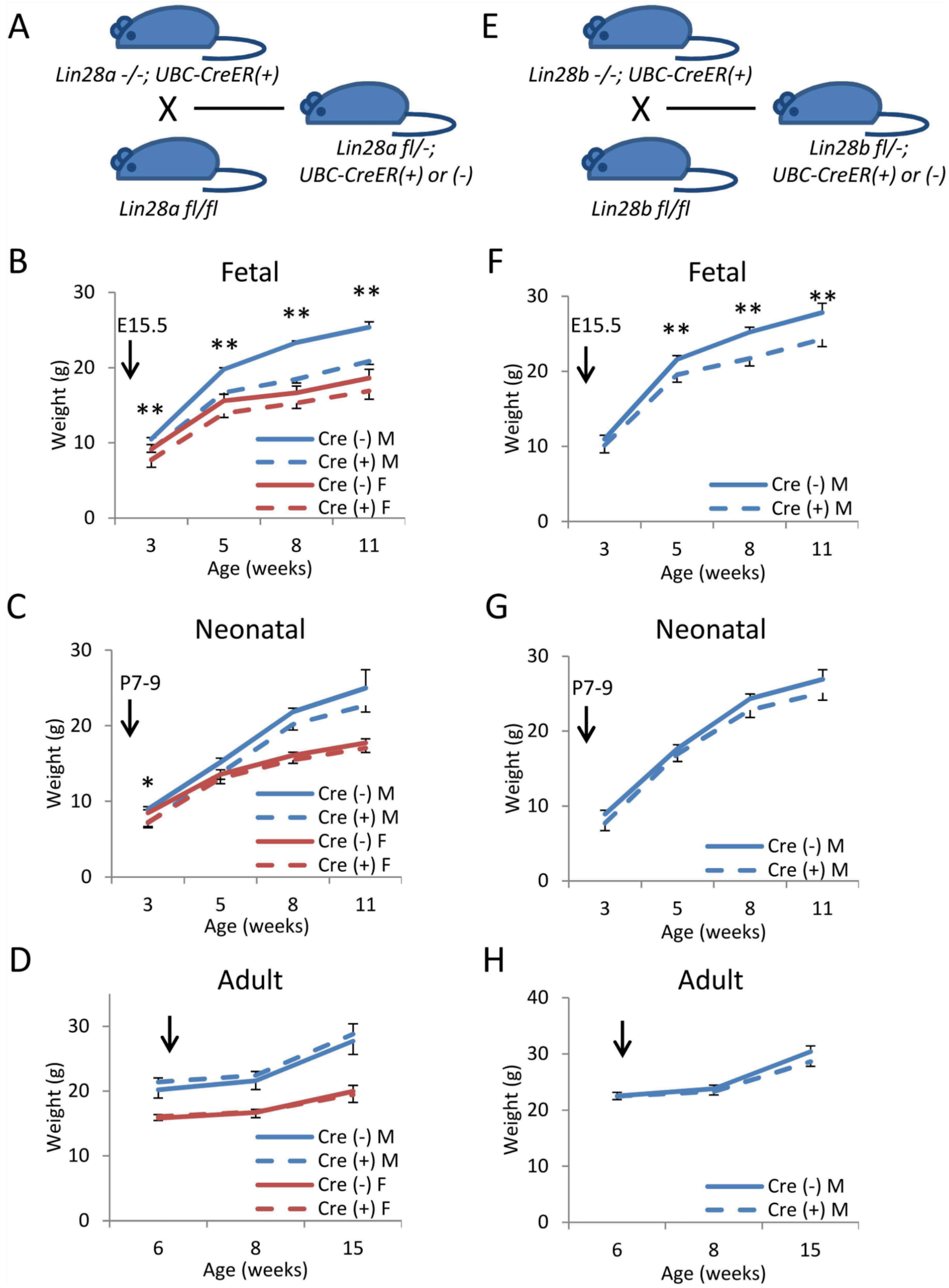

Figure 4. Fetal *Lin28a/b*, not neonatal or adult *Lin28a/b*, regulates postnatal growth

(A) Breeding strategy to test *Lin28a fl/−* mice at different ages. N=3–12. (B–D) Postnatal growth curves of *Lin28a fl/−; UBC-CreER (+)* vs. *Lin28a fl/−* mice. Body weights after tamoxifen (TAM) injections at (B) E15.5, (C) P7–9 and (D) 6 weeks. (E) Breeding strategy to test *Lin28b fl/−* mice at different ages. N=5–13. (F–H) Postnatal growth curves of *Lin28b fl/−; UBC-CreER (+)* vs. *Lin28b fl/−* mice. Body weights after TAM injections at (F) E15.5, (G) P7–9 and (H) 6 weeks. Arrows indicate ages at TAM injection. * $p<0.05$, ** $p<0.01$. Error bars represent SEM.

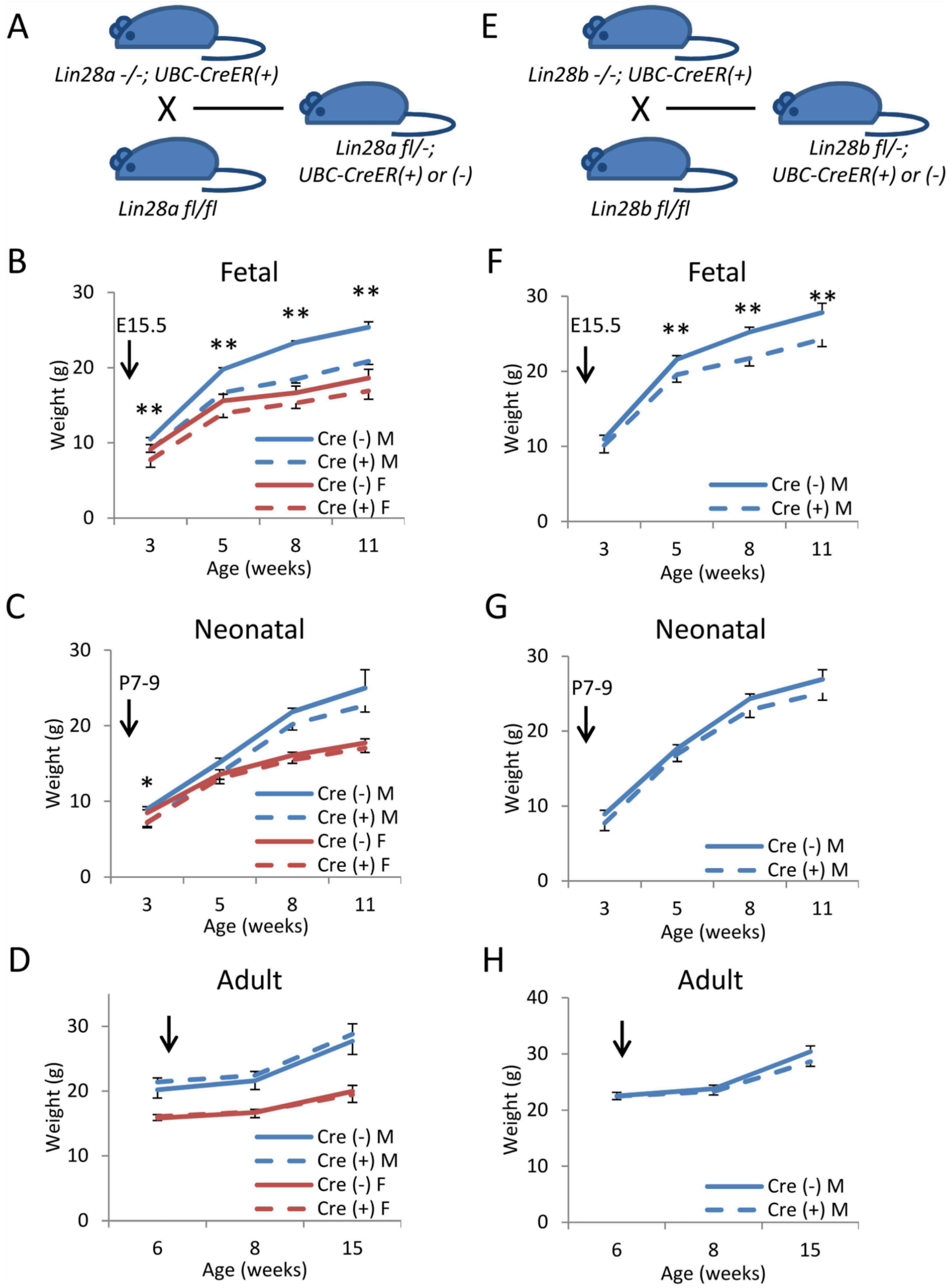

Figure 5. Glucose metabolism dysfunction in *Lin28a* KO and *Lin28b* KO mice

(A) Glucose tolerance tests (GTT) (N=9–10) and (B) Insulin tolerance tests (ITT) (N=8–11) of *Lin28b fl/fl; Myf5-Cre* mice. (C–E) Metabolomic changes in *Lin28a +/−* vs. −/− embryos at E10.5. (C) Glycolysis pathway. (D) Bioenergetics and redox balance. (E) Nucleotide synthesis. + p<0.1, * p<0.05, ** p<0.01. Error bars represent SEM.

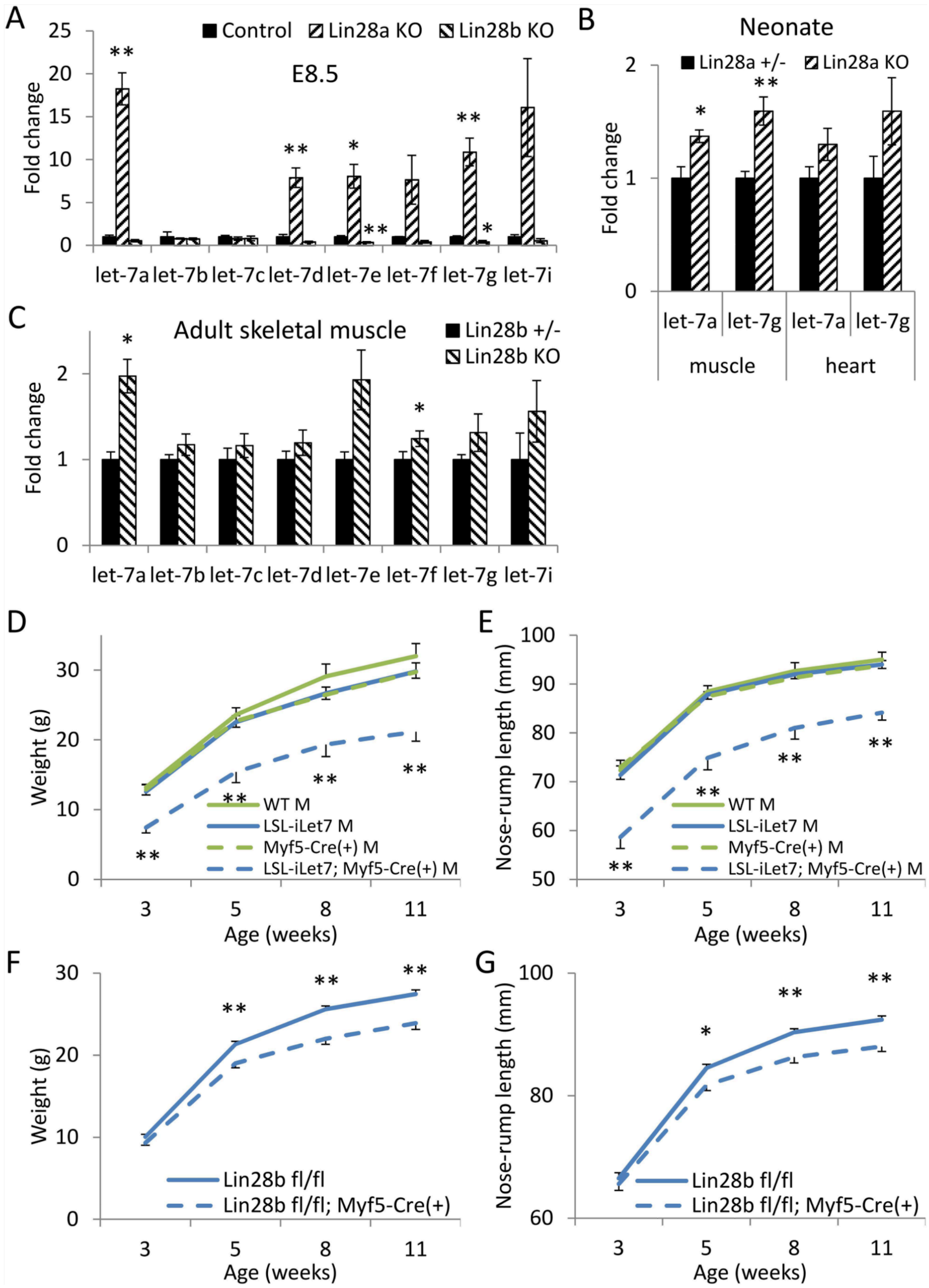

Figure 6. Muscle-specific *Lin28b/let-7* regulates postnatal growth

(A–C) *Let-7* levels in (A) *Lin28a +/−* vs. −/− E8.5 embryos, (B) *Lin28a +/−* vs. −/− neonatal muscles, and (C) *Lin28b +/−* vs. −/− adult skeletal muscles. N=3–5. (D–E) Postnatal growth curves of *LSL-iLet-7s; Myf5-Cre(+)* males given DOX from conception. N=6–13. Statistical significance was shown for *LSL-iLet-7s* (controls) vs. *LSL-iLet-7s; Myf5-Cre(+)* mice. (D) Body weights. (E) Body lengths. (F–G) Postnatal growth curves of *Lin28b fl/fl; Myf5-Cre* males. N=13–17. (F) Body weights. (G) Body lengths. * $p<0.05$, ** $p<0.01$. Error bars represent SEM.

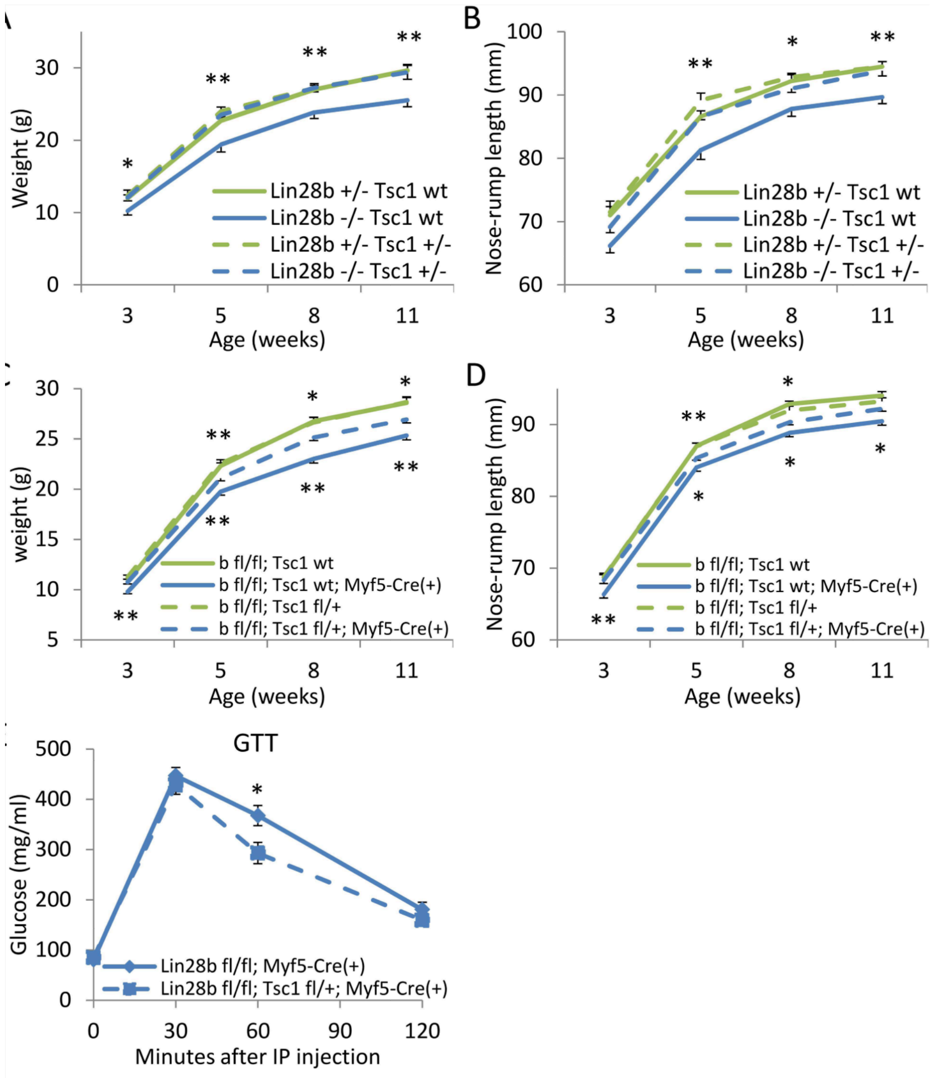

	Effect on growth					Effect on glucose metabolism
	Timing of expression				Expression in skeletal muscle	
	Embryonic	Fetal	Neonatal	Adult		
Lin28a	++	+	-	-	-	+
Lin28b	+/-	+	-	-	+	+

Figure 7. Tsc1/mTOR signaling in skeletal muscle can partially rescue aberrant programing of glucose metabolism and organismal growth in *Lin28b* KO mice

(A–B) Postnatal growth curves of *Lin28b* KO males, with or without *Tsc1* haploinsufficiency. N=6–14. (A) Body weights. (B) Body lengths. Statistical significance was shown for *Lin28b −/−; Tsc1 +/+* vs. *Lin28b −/−; Tsc1 +/−* mice. (C–D) Postnatal growth curves of *Lin28b fl/fl; Myf5-Cre* males, with or without *Tsc1* haploinsufficiency. N=21–29. (C) Body weights. (D) Body lengths. Statistical significance was shown for *Lin28b* fl/fl; *Tsc1 fl/+* vs. *Lin28b fl/fl; Tsc1 fl/−; Myf5-Cre(+)* mice on the top, and for *Lin28b* fl/fl; *Tsc1 +/+; Myf5-Cre(+)* vs. *Lin28b fl/fl; Tsc1 fl/−; Myf5-Cre(+)* mice on the bottom. (E) Glucose tolerance tests (GTT) of *Lin28b fl/fl; Tsc1 fl/+; Myf5-Cre* males. N=8–

11. (F) Summary of the timing and tissue of *Lin28a/b* expression and the effect on growth and glucose metabolism. Note that pink color denotes the positive effect on normal growth and glucose metabolism. The intensity of color and the number of + signs reflect the magnitude of the effect. "+/−" indicates that *Lin28b* has the effect on growth only if combined with *Lin28a* loss. * p<0.05, ** p<0.01. Error bars represent SEM.